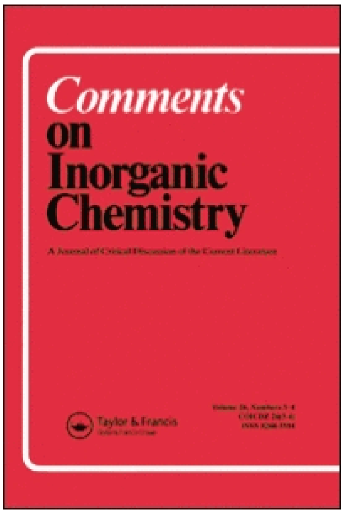

Comments on Inorganic Chemistry
Publication details, including instructions for authors and subscription information:
http://www.informaworld.com/smpp/title~content=t713455155

Alkaline-Earth Chalcogenolates: Exploration of Synthetic Strategies and Structural Chemistry

Karin Ruhlandt-senge[a]
[a] Department of Chemistry, Syracuse University and W. M. Keck Center for Molecular Electronics Syracuse, New York

To cite this Article Ruhlandt-senge, Karin(1997) 'Alkaline-Earth Chalcogenolates: Exploration of Synthetic Strategies and Structural Chemistry', Comments on Inorganic Chemistry, 19: 6, 351 — 385

To link to this Article: DOI: 10.1080/02603599708032746

URL: http://dx.doi.org/10.1080/02603599708032746

Alkaline-Earth Chalcogenolates: Exploration of Synthetic Strategies and Structural Chemistry

KARIN RUHLANDT-SENGE
Department of Chemistry,
Syracuse University and
W. M. Keck Center for Molecular Electronics
Syracuse, New York 13244-4100

Received May 12, 1997

Alkaline-earth chalcogenolates are important precursors in a variety of technical applications and in synthetic chemistry. Until recently, however, the number of well-characterized examples of alkaline-earth chalcogenolates was very small. During the last few years, several synthetic schemes have been explored, allowing the synthesis and characterization of a collection of alkaline-earth chalcogenolates. With a small family of target molecules in hand, it is now possible to further explore their use in synthetic chemistry and as precursor materials.

This article will highlight the important role of alkaline-earth chalcogenolates in a variety of applications, discuss critically different synthetic access routes in terms of accessibility, ease of reaction, yield and purity of the products, and will evaluate their structural chemistry in terms of structure-determining factors, such as type of ligand and donor, as well as the influence of the central metal and chalcogen atom.

Key Words: *alkaline-earth -thiolates, -selenolates and -tellurolates, synthetic and technical applications, synthetic strategies, structural studies*

1. INTRODUCTION

The discovery of superconducting ceramics and ferroelectric materials containing alkaline-earth ions such as $BaTiO_3$, $K_{0.4}Ba_{0.6}BiO_3$, YBa_2

Comments Inorg. Chem.
1997, Vol. 19, No. 6, pp. 351–385
Reprints available directly from the publisher
Photocopying permitted by license only

Cu_3O_{7-x}, $BaMg_{0.33}Ta_{0.66}O_3$, $Cu_3O_xM_2Tl$ (M = Ca, Ba), $CuO_4La_{1-x}Sr_x$ or $CuO_x Sr_yCa_n$[1–3] has revived research interest in the area of alkaline-earth chemistry. This work has focused mainly on the exploration of oxygen-containing alkaline-earth derivatives such as alkoxide, aryloxide, siloxide and β-diketonate species, producing a selection of soluble precursors allowing the formation of superconducting ceramics or ferroelectric materials by relatively simple procedures.[4–7]

In contrast, alkaline-earth analogs bearing heavier chalcogen ligands have received much less attention, which is surprising considering their importance as components in wide band gap semiconductors,[8–11] two-color IR optical windows[12] and phosphor materials.[13] Moreover, their use in synthetic chemistry has also been documented.[14–16]

So far, materials for wide band gap semiconductors have been based mainly on combinations of group IIB (Zn and Cd) and group VIA (S, Se, Te) elements and their mixed compounds.[17–20] As shown recently, the band gap of the conventional IIB-VIA materials can be widened significantly (by more than 1 eV) by alkaline-earth inclusion, as demonstrated with the incorporation of magnesium into ZnS/ZnSe phases. The novel quaternary ZnMgSSe material made possible the first continuous wave operation of blue-green laser diodes at room temperature. Importantly, the band gap extension can be controlled and depends on depositing conditions; so far, variations between 2.8 eV to 4.0 eV have been achieved by altering depositing conditions. These materials become especially important for the cladding layer materials in lasers, which are required to exhibit band gap energies of about 3 eV higher than that for the active layer.[8–11]

Functional II–VI magnesium-doped quaternary phases depend critically on precise control of material composition. Much work has been devoted towards the development of suitable routes and precursors, but the high purity II–VI materials needed for the production of blue-green lasers are still difficult to obtain, and further work is needed to develop alternative precursors and deposition techniques. Preliminary results indicate that the thermal decomposition of zinc and alkaline-earth chalcogenolates in the correct stoichiometric amounts yields pure, quaternary wide band gap materials. However, this route depends on a reliable supply of pure alkaline-earth chalcogenolates. One of the goals of our research is to explore synthetic schemes to alkaline-earth thiolates and selenolates and thoroughly investigate thermal decomposition processes.

The importance of alkaline-earth chalcogenolates extends towards applications in synthetic chemistry. Specifically, magnesium thiolates, selenolates and tellurolates are useful in metathesis reactions as shown with the synthesis of $Cp_2M(TeSi(SiMe_3)_3)_2$ (M = Ti, Zr).[14] The reagents are especially important in reactions with redox-sensitive metals; use of the corresponding alkali reagents often results in the formation of disulfides, selenides or tellurides and the reduced metal.[22] Moreover, the heterobimetallic thiolate $[Cu_4Mes_4][Mg(SAr)_2]_2$ (Mes = $2,4,6Me_3C_6H_2$, Ar = $SC_6H_4((R)\text{-}CH(Me)NMe_2)$),[15,16] comprised of two magnesium chalcogenolate units bound to a central tetranuclear cuprate moiety, has been related to Cu(I) catalyzed conjugate 1,4-addition of Grignard reagents to enones and other regio and stereospecific C–C bond forming processes.[15,16]

Despite the importance of molecular alkaline-earth derivatives in many areas of chemistry, only a few compounds exhibiting alkaline-earth thiolate, selenolate or tellurolate moieties have been mentioned.[14–16,23–29] Difficulties connected with heavy alkaline-earth chemistry are the high ionic character of the compounds, the large atomic radii of the metals and the low solubility of the dihalide precursors in organic solvents.[30–34] The greatest problem, however, might be the lack of suitable, alternative alkaline-earth starting materials, which would provide an easily accessible source of soluble alkaline-earth ions.[30–34] Moreover, the high sensitivity of many molecular alkaline-earth derivatives towards hydrolysis paired with high kinetic instability, especially if small groups are attached to the metal center, makes spectroscopic or crystallographic analysis of the target molecules difficult. Accordingly, any progress in heavy alkaline-earth chemistry depends on the development of feasible synthetic routes and alternative starting materials. Additionally, ligand and donor systems need to be tested in terms of their capacity to increase kinetic stability and steric saturation.

Alkaline-earth alkoxides, aryloxides and siloxides are fairly well studied due to their importance as precursors for the low temperature fabrication of high temperature superconductors and ferroelectric materials.[4–7] Examples include $Be(OMes*)_2(OEt_2)$[24] (Mes * = $2,4,6\text{-}tBu_3C_6H_3$), $[Mg(O(2,6\text{-}tBu_2C_6H_3))_2]_2$[34] and the heavier analogues $CaO(2,6\text{-}tBu_24\text{-}MeC_6H_2)_2(THF)_3$,[35] $[Ca_2(OSiPh_3)_4(NH_3)_4]$,[36] $[HBa_5(O)(OPh)_9(THF)_8]$,[37] $Ba_3(OSiPh_3)_6(THF)$[38] $[Ba_2(OSi(tBu)_3)_4(THF)]$[39] and many more.

Alkaline-earth thiolates and selenolates have been mentioned in the earlier literature,[40] but fully characterized species have only become available during the last few years. The first structurally characterized alkaline-earth chalcogenolate was a heteroorganocuprate $[Cu_4Mes_4][Mg(SAr)_2]_2$, displaying magnesium thiolate contacts, published in 1990 by van Koten *et al.*[15] In 1992, $Ca(TeSi(SiMe_3)_3)_2(THF)_4$ was reported simultaneously by the groups of Arnold[14] and Becker.[27] The first magnesium chalcogenolate, $Mg(TeSi(SiMe_3)_3)_2(THF)_2$, was also reported in 1992,[14] followed by the first beryllium thiolate, $Be(SMes^*)_2\,Et_2O$ in 1993.[24] Since then, a variety of synthetic access routes have been probed, allowing the synthesis of a small but increasing number of beryllium, magnesium, calcium, strontium and barium target molecules.

To date, structurally characterized alkaline-earth chalcogenolates include a small group of beryllium thiolates, namely the three coordinate $Be(SMes^*)_2THF$,[24] the four coordinate mixed amine/thiolate species $Be(SC_6F_5)_2(NH_3)(NH_2SiMe_3)$,[41] and $[\{Be(SPh)_2(py)(NH_3)\}_2\{18\text{-crown-}6\}]$[41] and the solvent-separated triple-ion $[Be(HMPA)_4][SCPh_3]_2$ (HMPA = hexamethylphosphoramide).[41] A fair number of magnesium chalcogenolates have been synthesized and characterized, including the first base-free, three coordinate magnesium thiolate $[Mg(S(2,4,6\text{-}Ph_3C_6H_2))_2]_2$,[25] and a variety of four and five coordinate species such as $Mg(SMes^*)_2(Et_2O)_2$,[25] $Mg(TeSi(SiMe_3)_3)_2(THF)_2$,[14] $Mg(SC_6F_5)_2(py)_3$[42] and the intramolecular stabilized dimer $[Mg\{S(C_6H_4\text{-}2\text{-}CH_2NMe_2)\}_2]_2$.[26] Recently, a small group of six coordinate target molecules was prepared and examined, including $Mg(SPh)_2(py)_4$,[42] $Mg(S2\text{-}NC_5H_4)_2(py)_2$[42] and the trimeric pyridine adduct $[Mg_3(\eta^2SPh)_6(py)_6]$.[42] Other examples include the first anionic magnesium thiolate complex $[lutidineH]_2[Mg(SC_6F_5)_4]$[42] and the solvent-separated magnesium thiolate $[Mg(15\text{-crown-}5)(THF)_2][SMes^*]_2$.[42] The number of heavier alkaline-earth target molecules is much smaller. Examples include the octahedrally coordinate $Ca(SC_6F_5)_2(py)_4$,[43] the eight-coordinate contact pair $Ca(18\text{-crown-}6)(SMes^*)_2$,[43] the solvent-separated triple-ion $[Ca(18\text{-crown-}6)(NH_3)_3][SMes^*]_2$[43] and the tellurolate $Ca(TeSi(SiMe_3)_3)_3$ $(THF)_4$.[14,27] Only a few strontium derivatives have been mentioned. $Sr(EMes^*)_2(THF)_4$,[28] (E = S, Se) and $Sr(SeSi(SiMe_3)_3)_2\,(TMEDA)_2$,[29] all display six-coordinate metal centers. Utilization of the strong donor HMPA in combination with crown-ether made possible the isolation of the solvent-separated triple-ion $[Sr(18\text{-crown-}6)(HMPA)_2][SMes^*]$.[44] Structural data of strontium tellurolates are, to the best of our knowledge, not available. Only a few chalcogenolate complexes of barium have been reported; and data are available for the unusual thiolate $[Ba(SMes^*)(18\text{-crown-}6)$ $(HMPA]$ $[SMes^*]$[45] described as an intermediate between contact and a solvent-separated triple-ion. In addition, a small group of monomeric and dimeric barium selenolates[45] and the tellurolate $Ba(TeSi(SiMe_3)_3)_2(py)_5$[29] have been prepared.

2. SYNTHETIC METHODS

During the last few years much work has been devoted towards the development of synthetic routes allowing the isolation of pure alkaline-earth chalcogenolates. The goal was to develop reliable, reproducible, high-yielding reactions, which would result in the synthesis of a wide variety of target compounds. So far, several different reaction schemes have been developed and tested; Table I summarized the different synthetic routes.

Alkaline-earth chalcogenolates are sensitive to oxygen and moisture and must be handled and stored under strict anaerobic conditions. Generally, use of Schlenk-line and/or dry-box techniques and vigorously dried and degassed reagents and solvents are necessary. Upon formation and isolation, the target molecules are stable and can be stored under inert gas over extended time periods without detectable decomposition.

TABLE I

Synthetic routes to alkaline-earth chalcogenolates.

Type of Reaction	Equation	Used For
Transamination	$Ae(N(SiMe_3)_2)_2 + 2\ HER \rightarrow Ae(ER)_2 + 2\ HN(SiMe_3)_2^{a}$	Be, Mg, Ca, Sr, Ba SR, SeR, TeR
Salt Elimination/ Metathesis	$AeX_2 + 2\ AER \rightarrow Ae(ER)_2 + 2\ AX^{b}$	Be, Mg, Sr SR, SeR
Alkane Elimination	$(Bu)_2Ae + 2\ HERBuH \rightarrow Ae(ER)_2 + 2$	Mg SR, SeR, TeR
Metallation	$Ae_{act.} + 2\ HER \rightarrow Ae(ER)_2 + H_2^{c}$ $Ae_{act.} + REER \rightarrow Ae(ER)_2$	Ca, Sr, Ba SR, SeR
Transmetallation	$Ae + Hg(ER)_2 \rightarrow Ae(ER)_2 + Hg$	Mg, TeR
Chalcogen Insertion	$R_2Ae + {}_{2/8}\ S_8 \rightarrow Ae(SR)_2$	Mg, SR

[a] E = S, Se, Te, R = alkyl, aryl, silyl.

[b] X = halide, A = Li, Na, K.

[c] Activation of alkaline-earth metals can be achieved by different routes; most efficient is the solvation of the metals in predried liquid ammonia.

2.1. Transamination

This versatile route allows the preparation of the target molecules in a variety of solvent and ligand systems in high yield and purity. The reaction scheme involves the treatment of alkaline-earth amide[46] with thiols, selenols and tellurols (see Eq. (1)). The resulting amine can be removed in vacuum.

$$[Ae(N(SiMe_3)_2)_2]_2 + 4\ HER \rightarrow 2\ Ae(ER)_2 + 4\ HN(SiMe_3)_2$$

$$(Ae = \text{alkaline-earth metal}, E = S, Se, Te, R = \text{alkyl, aryl, silyl}) \quad (1)$$

This reaction route has been used successfully for the synthesis of a variety of target compounds, such as $[Mg(STriph)_2]_2$ (Triph = 2,4,6Ph$_3$C$_6$H$_2$),[25] $Mg(SMes^*)_2(OEt_2)_2$,[25] $Mg(SeMes^*)_2(THF)_2$,[25] $Ca(SC_6F_5)_2(py)_4$ (py = pyridine),[43] $Ca(TeSi(SiMe_3)_3)_2(THF)_4$,[14,27] $Sr(SeSi(SiMe_3)_3)_2(TMEDA)_2$[29] (TMEDA = N,N,N′,N′-tetramethylethylenediamine), $Ba(TeSi(SiMe_3)_3)_2(py)_5$[29] and others.

The transamination route allows a great deal of synthetic flexibility: both donor and non-donor solvents can be used, and a large variety of thiols, selenols and tellurols can be employed. The byproduct, $HN(SiMe_3)_2$, is easily removed from the reaction mixture. One disadvantage of transamination involves the occasional incomplete amide exchange. For example, the reaction of $[Mg(N(SiMe_3)_2)_2]_2$ with two equivalents of HSTrip (Trip = 2,4,6-iPr$_3$C$_6$H$_2$) results in the formation of the mixed amide thiolate trimer $[Mg_3(\eta^2STrip)_4(\eta^1N(SiMe_3)_2)_2]$ in low yields.[47] Variation of reaction conditions and stoichiometry does not allow for the isolation of the amide-free thiolate. Another disadvantage of this reaction scheme is the need to prepare alkaline-earth amides, often a time consuming, low yielding process.[46]

2.2. Salt Elimination/Metathesis

Alkaline-earth chalcogenolates are also accessible by the reaction of alkaline-earth halides with alkali chalcogenolates (Eq. (2)):

$$AeX_2 + 2\ AER \rightarrow Ae\ (ER)_2 + 2\ AX$$

$$(X = \text{halogen}, A = \text{alkali metal}) \quad (2)$$

Only a few target compounds have been prepared using this method since the disadvantages of this methodology far outnumber the ready availability of alkali chalcogenolates and alkaline-earth halides. Arnold and Gindelberger describe the reaction between lithium tellurolate and magnesium bromide as resulting only in intractable mixtures,[29] an observation generally shared in our group. Problems associated with this reaction route are related to the need for fine-tuning of alkali chalcogenolate reactivity. For example, the reaction of $MgBr_2$ with two equivalents of $Li(THF)_3SMes^*$ or $Li(THF)_3SeMes^*$ results in the formation of magnesium thiolate or selenolate etherates.[25] In contrast, the analogous reaction of $CaBr_2$ with two equivalents of $Li(THF)_nSTrip$ results in the isolation of an adduct between unreacted $CaBr_2$ and LiBr, $[Ca(THF)_2(\eta^2Br)_4(\eta^4Li)_2(THF)_4]$.[43] Apparently, the reaction takes place to some degree, as indicated by the formation of LiBr; however, it was not possible to isolate the target molecule from the reaction mixture. Interestingly, the reaction of SrI_2 with two equivalents of lithium thiolate or selenolate led to isolation of starting materials, while employment of the potassium reagents allowed the isolation of $Sr(EMes^*)_2(THF)_4$ (E = S, Se) in high yields.[28] To date, only a few compounds have been prepared using this methodology, and it is therefore impossible to recommend specific reagents or reaction conditions.

Another major disadvantage of salt elimination involves solvent selection, which is limited to etheral solvents due to the insolubility of the dihalide starting materials in hydrocarbons.[30–33] Furthermore, the low solubility of alkaline-earth chlorides, even in etheral solutions, requires the use of alkaline-earth bromides or iodides. The high solubility of alkali bromides or iodides in ethers, however, renders the alkali halide difficult to remove from the reaction mixture. Thus, intractable reaction mixtures are commonly observed.

Still, a small number of target molecules have been prepared using this synthetic methodology. Examples include the beryllium thiolate $Be(SMes^*)_2(OEt_2)$,[24] the magnesium derivatives $Mg(SMes^*)_2(OEt_2)_2$[25] and $Mg(SeMes^*)_2(THF)_2$,[25] as well as the strontium species $Sr(SMes^*)_2(THF)_4$ and $Sr(SeMes^*)_2(THF)_4$.[28]

2.3. Alkane Elimination

This reaction scheme has been used extensively for the synthesis of magnesium chalcogenolates bearing a wide variety of ligands and donors. The magnesium starting material is commercially available as a 1 : 1 mixture of n-butyl and sec-butyl magnesium, $(n\text{-}Bu/sec\text{-}Bu)_2Mg$ in heptane (Aldrich), or as a dibutyl magnesium solution in diethylether (Fluka). The reaction of dibutyl magnesium with two equivalents of thiols, selenols or tellurols (see Eq. (3)) produces the target molecules in excellent yield and purity.

$$(Bu)_2Mg + 2\,HER \rightarrow Mg(ER)_2 + 2BuH$$
$$(E = S, Se, Te) \qquad (3)$$

The primary advantage of this method is the wide synthetic flexibility: a large variety of solvents, donors and ligands can be utilized. Moreover, the reaction proceeds cleanly within a short time, and purification steps can be avoided due to the gaseous nature of the byproducts. Examples of compounds prepared using this route are $[Mg(STriph)_2]_2$,[25] $Mg(SMes^*)_2(OEt_2)_2$,[25] $Mg(SPh)_2(py)_4$,[42] $Mg(SC_6F_5)_2(py)_3$,[42] the magnesiate $[2,6\ lutidineH]_2[Mg(SC_6F_5)_4]$,[42] the solvent-separated triple-ion $[Mg(15\text{-}crown\text{-}5)_2(THF)_2][SMes^*]_2$,[42] the selenolates $Mg(SeSi(SiMe_3)_3)_2(TRMPSI)$[29] (TRMPSI = tris(dimethylphosphinomethyl)-t-butylsilane), $Mg(SeMes^*)_2(THF)_2$[25] and the tellurolate $Mg(TeSi(SiMe_3)_3)_2(THF)_2$.[14,29] Since diorgano derivatives of the heavier alkaline-earth elements are not readily available, this method is currently limited to magnesium and beryllium complexes, though no beryllium chalcogenolates have been synthesized employing this route.

2.4. Metallation

The reaction of alkaline-earth metals with phenols in the presence of ammonia has been utilized to synthesize a number of alkaline-earth aryloxides and siloxides,[7,36–39] but only recently has this method been extended for the preparation of the heavier group VIA analogues (Eq. (4)).[43–45] Alternatively, the reaction of lanthanide metals with diselenides or -tellurides produced lanthanide-selenolates and -tellurolates in excellent yields and purity.[48] Very recently, Ruhlandt-Senge and coworkers showed the extension of this method to the corresponding alkaline-earth analogues (Eq. (5)).[45]

$$Ae_{act.} + 2HER \rightarrow Ae\,(ER)_2 + H_2 \qquad (4)$$

$$Ae_{act.} + 2HER \rightarrow Ae\,(ER)_2 + H_2$$
$$(act. = activated)$$
$$Ae = Ca, Sr, Ba,$$
$$E = S, Se, Te \qquad (5)$$

A critical requirement in the reaction of alkaline-earth metals with thiols, selenols or tellurols is to provide highly activated alkaline-earth metal. Lappert *et al.* reported the successful synthesis of calcium phenolate by reacting pyrophoric calcium (co-condensation activated metal) with HO-2,6tBu$_2$-4MeC$_6$H$_2$ in THF.[35] Interestingly, the reaction failed if hydrocarbon solvents were employed, indicating a strong solvent dependability of the reaction. As shown with the synthesis of various alkaline-earth alkoxides, siloxides and aryloxides,[7,36–39] and recently with several thiolates and selenolates,[43–45] that the solvent dependability can be overcome by addition of dry, liquid ammonia to the reaction mixture. Reaction (5) is especially attractive for the preparation of selenolate and tellurolate derivatives, since the reduction of the di-selenide or -telluride to the highly air-sensitive selenol or tellurol, a low yielding reaction, can be avoided. Examples of compounds synthesized using metallation are [Ca(18-crown-6)(NH$_3$)$_3$][SMes*]$_2$,[43] Ca(SMes*)$_2$ (18-crown-6),[43] [Sr(18-crown-6) (HMPA)$_2$][SMes*]$_2$,[44][Ba(SMes*) (18-crown-6)HMPA][SMes*],[45] Ba(SEMes*)$_2$(THF)$_4$,[45] E = S; Se the dimeric [Ba(SeTrip)$_2$(py)$_3$(THF)]$_2$[45] and the eight coordinate Ba(SeTrip)$_2$ (18-crown-6).[45]

2.5. Transmetallation

As shown with the synthesis of Mg(TeSi(SiMe$_3$)$_3$)$_2$(THF)$_2$,[14,29] transmetallation routes can be used to obtain alkaline-earth chalcogenolates (Eq. (6)).

$$\mathrm{Ae + Hg(TeR)_2 \quad \rightarrow \quad Ae\,(TeR)_2 + Hg} \qquad (6)$$

In the above reaction, mercury tellurolate was reacted with an excess of magnesium powder to yield the target compound.[14,29] A major disadvantage of this method is the need to synthesize the mercury reagents.[49] Also, activated alkaline-earth metal powder is required to enable a smooth, high-yielding reaction. The synthetic sequence is therefore time consuming and, so far, untested for the heavier alkaline-earth analogues.

2.6. Chalcogen Insertion into Metal–Carbon Bond

It has been long known that magnesium thiolates are accessible by sulfur insertion into the metal carbon bond, as employed in the synthesis of thiols, when elemental sulfur is reacted with Grignard reagents.[50]

However, only recently was the first magnesium thiolate isolated and fully characterized using this route.[26] The dimeric intramolecularly stabilized magnesium thiolate $[Mg\{S(C_6H_4\text{-}2\text{-}CH_2NMe_2)\}_2]_2$ was prepared by treating the diorganomagnesium precursor with elemental sulfur in THF (Eq. (7)).[26]

$$R_2Mg + 2/8\ S_8 \rightarrow Mg\,(SR)_2 \qquad (7)$$

The major advantage of this route is the lack of unwanted byproducts. The need to prepare the diorganomagnesium derivative, though, is a major disadvantage. Moreover, this method is currently limited to beryllium and magnesium derivatives, due to difficulties in obtaining organocalcium, strontium and barium derivatives.

3. STRUCTURAL INVESTIGATIONS

3.1. Beryllium Thiolates

Beryllium chemistry has received little attention, most likely due to the high toxicity of beryllium and its compounds.[30,51] Not surprisingly, this lack of attention is reflected in the small number of structurally characterized beryllium species,[52] especially those displaying bonds with elements located in row three and below in the periodic table. Accordingly, the number of well characterized beryllium thiolates is very small, and to the best of our knowledge, no structural data on beryllium selenolates or tellurolates are available. Examples of compounds displaying beryllium sulfur contacts include the three-coordinate thiolate $Be(SMes^*)_2THF$,[24] shown in Fig. 1, and a family of four-coordinate species including bis(dialkyldithiocarbamato)beryllium $Be\{S_2N(i\text{-}Pr)\}_2$,[53] the mixed beryllium thiolate amines $Be(SC_6F_5)_2(NH_3)(NH_2SiMe_3)$ and $[\{Be(SPh)_2(py)(NH_3)\}_2\{18\text{-crown-}6\}]$[41] (Fig. 2) and the unusual solvent-separated triple-ion $[Be(HMPA)_4][SCPh_3]_2$[41] (Fig. 3). Table II summarizes important structural parameters displayed in the thiolates.

The commonly observed structural motif in beryllium chemistry is a tetrahedral coordination environment as observed in the majority of beryllium thiolates. The mixed amine thiolate derivative $Be(SC_6F_5)_2(NH_3)(NH_2SiMe_3)$[41] exhibits a tetrahedral beryllium center ligated by two pentafluorothiolate ligands in addition to one ammonia and one

TABLE II

Selected structural parameters for beryllium thiolates.

Compound	Ae-E (Å)	Ae-Donor (Å)	S-C_{ipso} (Å)	C.N. (metal)	Ref.
Be(SMes*)$_2$THF	1.991(7), 1.987(8)	1.590(7)	1.799(6), 1.810(5)	3	24
Be(SC$_6$F$_5$)$_2$(NH$_3$)(NH$_2$SiMe$_3$)	2.098(7), 2.128(7)	1.738(9), 1.744(8)	1.754(5), 1.750(5)	4	41
[{Be(SPh)$_2$(py)(NH$_3$)}$_2${18-crown-6}]	2.103(3), 2.100(3)	1.724(4), 1.779(4)	1.770(2), 1.771(3)	4	41
	2.095(3), 2.086(3)	1.731(4), 1.778(4)	1.764(3), 1.768(2)		
[Be(HMPA)$_4$][SCPh$_3$]$_2$	–	1.54(1)– 1.63(1)	1.78(1), 1.79(1)	4	41

Abbreviations: Mes* = 2,4,6-tBu$_3$C$_6$H$_2$, HMPA = hexamethylphosphoramide, py = pyridine.

trimethylsilylamine donor molecule. The crown-ether coordinate [{Be(SPh)$_2$(py)(NH$_3$)}$_2${18-crown-6}] (Fig. 2) exhibits two identical four coordinate beryllium centers, comprised of two phenylthiolate ligands, one pyridine and one NH$_3$ donor connected via NH$_3$ crown-ether hydrogen bonds. The common motif between the mixed amine/thiolate species is a N–Si bond cleavage reaction, a result of iterative protonation

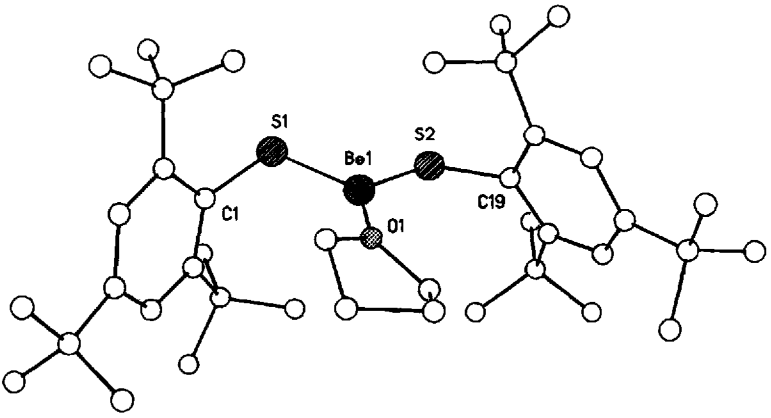

FIGURE 1 The crystal structure of Be(SMes*)$_2$ THF (Ref. 24). Hydrogen atoms have been omitted for clarity.

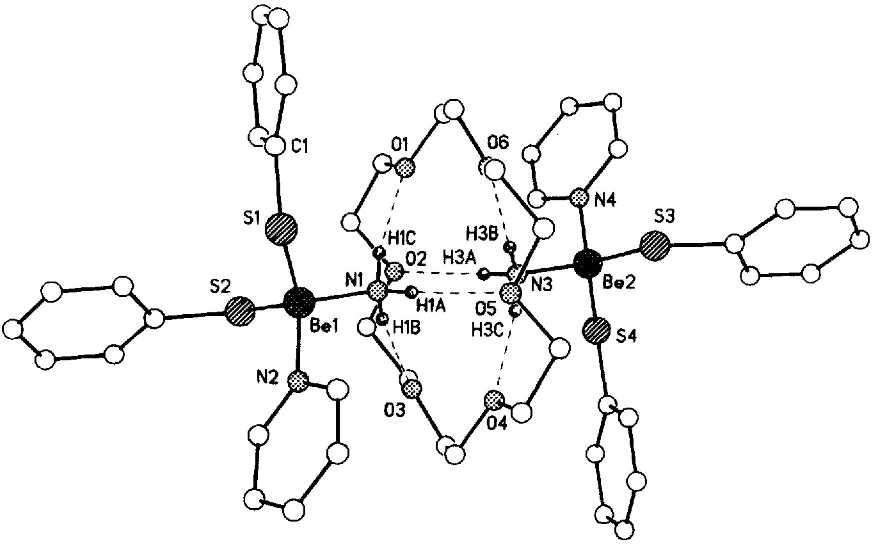

FIGURE 2 The crystal structure of $[\{Be(SPh)_2(py)(NH_3)_2\}\{18\text{-crown-}6\}]$ (Ref. 41). Hydrogen atoms with the exception of those bound to the crown-ether have been removed for clarity.

of the product $HN(SiMe_3)_2$ by HSPh and HSC_6F_5, yielding H_2NSiMe_3 and NH_3, respectively. The solvent-separated triple-ion $[Be(HMPA)_4][SCPh_3]_2$ shown in Fig. 3, available by addition of the strong donor HMPA to a mixture of $Be\{N(SiMe_3)_2\}_2$ and $HSCPh_3$, contains a tetrahedrally coordinate Be^{2+} cation. Also present are two uncoordinated STrityl anions; there are no close interactions between cations and anions. The formation of this triple-ion may be the result of weak interactions between the small, hard beryllium cation and the soft thiolate sulfur anions. Apparently, the interaction of the small beryllium ion with the harder oxygen donors is favored. Additionally, the substantial partial negative charge on the HMPA oxygen[54] stabilizes the dicationic beryllium center. The distorted trigonal planar coordination geometry at beryllium observed in $Be(SMes^*)_2THF$[28] (Fig. 1) is observed only if the steric requirement of the ligand is large. Comparison of beryllium sulfur contacts in the three coordinate $Be(SMes^*)_2THF$,[28] with the four-coordinate $Be(SC_6F_5)_2(NH_3)(NH_2SiMe_3)$,[41] $[\{Be(SPh)_2(py)(NH_3)\}_2\{18\text{-crown-}6\}]$[41] and $Be\{S_2N(i\text{-}Pr)\}_2$[48] reveals slightly shorter bond lengths for the three-coordinate compound, 1.98(1) Å (avg.) vs. 2.11(1) Å (avg.),

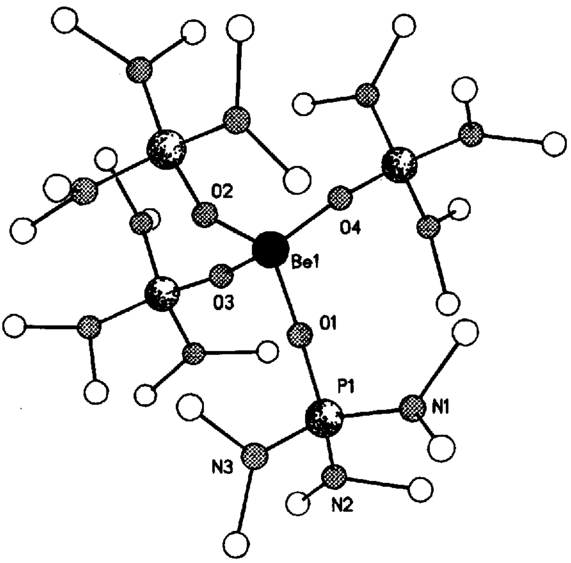

FIGURE 3 The crystal structure of $[Be(HMPA)_4][SCPh_3]_2$ (Ref. 41). Only the cation $[Be(HMPA)_4]^{2+}$ is shown; hydrogen atoms have been omitted for clarity.

2.096(1) Å avg. and 2.098(9) Å (avg.), which is most likely due to the reduced coordination number at beryllium. The experimental values observed for the beryllium sulfur bond lengths correlate well with the calculated Be–S distances in monomeric $Be(SH)_2$ (1.954 Å).[55]

3.2. Magnesium Thiolates, Selenolates and Tellurolates

Magnesium chalcogenolates comprise the largest group of well-characterized alkaline-earth chalcogenolates. Table III summarizes selected structural parameters for magnesium chalcogenolates.

The number of reported donor-free magnesium thiolates, selenolates or tellurolates remains very small; to date only one compound, the dimeric $[Mg(STriph)_2]_2$ has been structurally characterized. Recently, the two coordinate magnesium thiolate $Mg(S2,6Mes_2C_6H_3)_2$[56] (Mes = $2,4,6Me_3C_6H_2$) was mentioned in the literature, but structural evidence supporting its presumably monomeric nature is not available. It is postulated that the monomeric motif of this compound is made possible by the use of the very bulky $S2,6Mes_2C_6H_3$ ligand. Reduction of ligand size and employment of the -STriph ligand resulted in the isolation of the

TABLE III

Selected structural parameters for magnesium thiolates and selenolates.

Compound	Ae-E (Å)	Ae-Donor (Å)	S-C_{ipso} (Å)	C.N. (metal)	Ref.
$[Mg(STriph)_2]_2$	$2.466(5)_{br}$, $2.458(5)_{br}$ $2.349(5)_t$	–	1.775(6)	3 (+3)	25
$Mg(SMes^*)_2(Et_2O)_2$	2.382(2), 2.392(2)	2.074(3), 2.065(3)	1.798(4), 1.807(4)	4	25
$Mg(SeMes^*)_2(THF)_2$	2.536(3), 2.539(3)	2.021(5), 2.013(5)	1.958(9), 1.957(10)	4	25
$Mg(TeSi(SiMe_3)_3)_2(THF)_2$	2.720(1), 2.714(1)	2.035(2), 2.038(2)	2.504(1), 2.504(1)	4	14, 29
$[(CuMes)_4(\mu\text{-}SAr)_2(MgSAr)_2]$	$2.427(4)_{br}$, $2.375(4)_t$	2.186(8), 2.180(8)		4	15
$[C_7H_9NH]_2[Mg(SC_6F_5)_4]$	2.416(3), 2.464(3) 2.432(3), 2.483(3)	–	1.753(7), 1.756(7) 1.751(8), 1.757(6)	4	42
$Mg(SC_6F_5)_2(py)_3$	2.476(4), 2.505(4)	2.139(7), 2.184(6) 2.191(6)	1.752(8), 1.757(7)	5	42
$Mg(SeSi(SiMe_3)_3)_2TRMPSI$	2.483(8), 2.500(8)	2.65(1), 2.66(1)	2.266(7), 2.300(7)	5	29
$[Mg(SC_6H_4\text{-}2\text{-}CH_2NMe_2)_2]_2$	$2.519(2)_{br}$, $2.578(2)_{br}$ $2.446(2)_t$	2.252(3), 2.239(4)	1.761(4), 1.770(4)	5	26
$Mg(SPh)_2(py)_4$	2.6247(5)	2.220(2), 2.360(2)	1.77(2)	6	42
$Mg(SNC_5H_4)_2(py)_2$	2.612(2), 2.613(2)	2.159(3), 2.173(3) 2.188(3), 2.227(3)	1.763(3), 1.748(3)	6	42
$[Mg_3(\eta^2SPh)_6(py)_6]$	2.596(1), 2.613(1) 2.628(1)	2.205(2), 2.231(2) 2.234(2)	1.770(2), 1.779(2) 1.776(2)	6	
$[Mg(15\text{-}crown\text{-}5)(THF)_2][SMes^*]_2$	–	$2.088(3)^a$, $2.098(3)^a$ $2.118(4)^b$, $2.160(4)^b$ $2.172(4)^b$, $2.189(4)^b$ $2.195(4)^b$	1.766(5), 1.779(5)	7	42

Abbreviations: Mes* = 2,4,6-$tBu_3C_6H_2$, Triph = 2,4,6$Ph_3C_6H_2$, py = pyridine, Mes = 2,4,6$Me_3C_6H_2$, Ar = $C_5H_4(CHMeNMe_2)$, TRMPSI = tris(dimethylphosphinomethyl)-*tert*-butylsilane, t = terminal, br = bridging.

[a] Mg–THF contacts, b = Mg–crown-ether contacts.

dimeric $[Mg(STriph)_2]_2$,[25] exhibiting rare, three-coordinate magnesium centers. $[Mg(STriph)_2]_2$, shown in Fig. 4, is dimeric with thiolato bridges and terminal thiolato groups. The two halves of the dimer are related by a center of symmetry, such that the core Mg_2S_2 array is required to be planar. The $\{MgS_3\}$ coordination, however, deviates from planarity with the sum of S–Mg–S angles of 340.8(1)°. The $Mg–S_{bridging}$ distances are, as expected, longer than the $Mg–S_{terminal}$ bond length with values differing by 0.12 Å (2.349(5) vs. 2.466(5) Å). There are some short interactions between the magnesium and the carbon atoms of the ortho-phenyl ligands, the shortest being 2.555 and 2.797 Å. It is believed that the weak π-type interactions between ligand and metal make possible the dimeric nature of this compound.

In contrast to the small number of donor-free magnesium chalcogenolates, a much larger variety of donor containing species is known. Here, a range of coordination numbers varying between four and seven is observed, mainly depending on ligand size and, to a lesser extent, the donors. Complexes exhibiting a coordination number of four are

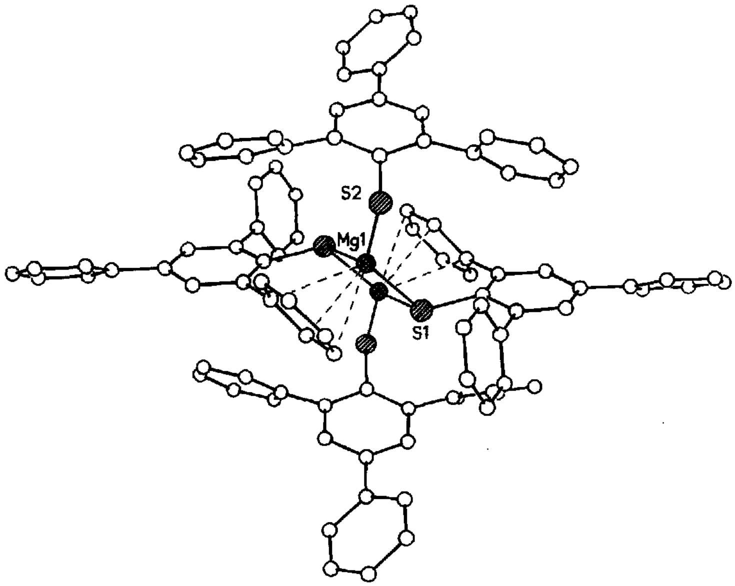

FIGURE 4 The crystal structure of the donor-free dimer $[Mg(STriph)_2]_2$ (Ref. 25). The dotted lines indicate π-type bonds between magnesium and the ortho-phenyl groups of the ligand; hydrogen atoms have been omitted for clarity.

generally observed if bulky ligands and a donor are utilized. Examples include $Mg(SMes^*)_2(OEt_2)_2$,[25] shown in Fig. 5, $Mg(SSiPh_3)_2$ $(HMPA)_2$,[42] $Mg(SeMes^*)_2(THF)_2$,[25] $Mg(SeSi(SiMe_3)_3)_2TRMPSI$[29] and Mg(TeSi $(SiMe_3)_3)_2(THF)_2$.[14,29] Other four-coordinate magnesium chalcogenolates include the bimetallic aggregate $[Mg_2(SC_6H_4((R)\text{-}CH(Me)NMe_2))_4Cu_4$ $(Mes)_4]$,[15,16] and the first anionic tetrachalcogenolato magnesiate $[lutidineH]_2[Mg(SC_6F_5)_4]$,[42] shown in Fig. 6. Related, four-coordinate species exhibiting magnesium-sulfur or -selenium contacts are the complexes $[Tp^{p\text{-}Tol}]MgSH$, $[Tp^{p\text{-}Tol}]MgSeH$ and $\{[Tp^{p\text{-}tol}]Mg\}_2Se$ ($Tp^{p\text{-}Tol}$ = tris(3-*p*-tolylpyrazolyl)hydroborato).[57] Magnesium chalcogenolates displaying higher coordination numbers are commonly observed if the steric requirement of the ligand is reduced, as demonstrated with the five coordinate dimeric, intramolecularly stabilized dimer $[Mg(SC_6H_4\text{-}2\text{-}CH_2$ $NMe_2)_2]_2$ [26] (Fig. 7a) and the monomeric $Mg(SC_6F_5)_2(py)_3$ (Fig. 7b).[39] Replacement of the $SC_6F_6^-$ ligand by the slightly smaller phenylthiolate, SPh^-, results in the formation of the octahedral complex $Mg(SPh)_2$ $(py)_4$ (Fig. 8a).[42] The conformationally related, distorted octahedral Mg(S2-$NC_5H_4)_2(py)_2$[42] (Fig. 8b) is observed if the intramolecular stabilizing

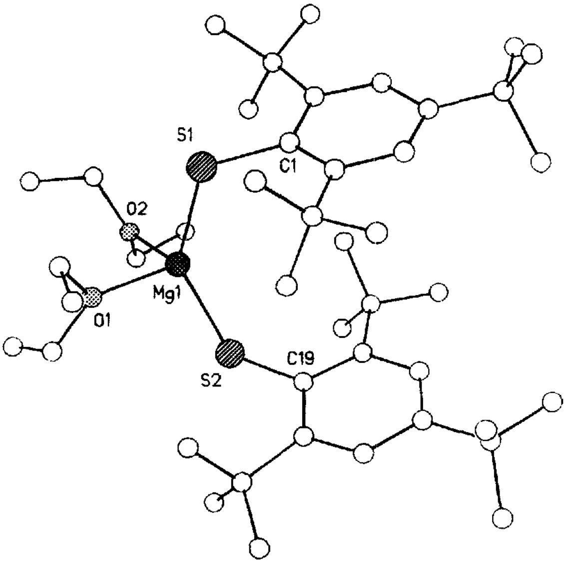

FIGURE 5 The crystal structure of $Mg(SMes^*)_2(Et_2O)_2$ (Ref. 25): hydrogen atoms have been omitted for clarity.

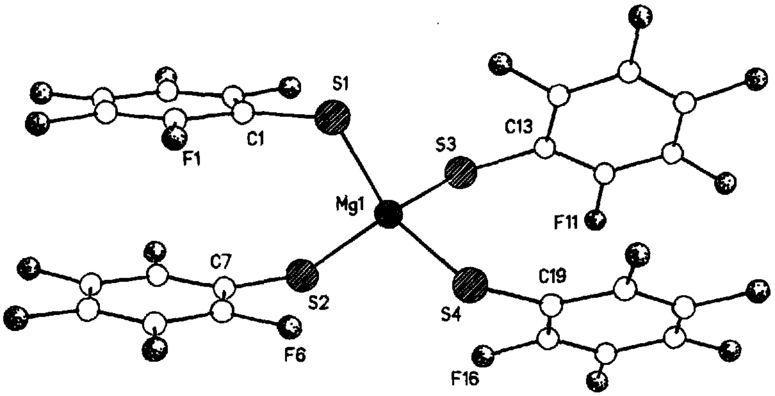

FIGURE 6 The crystal structure of the anionic magnesium thiolate [2,6 lutidineH]$_2$ [Mg(SC$_6$F$_5$)$_4$] (Ref. 42). Only the anion is shown.

pyridinethiolate ligand is used in combination with pyridine. Limiting the amount of pyridine and utilization of phenylthiol afforded the trimeric species [Mg$_3$(η^2SPh)$_6$(py)$_6$] (Fig. 9), exhibiting three octa-hedrally coordinate metal centers, the central magnesium unit is bound to six bridging sulfur atoms, two of the outer units are bound to three bridging sulfur atoms and three terminal pyridine molecules, resulting in a ligand donor stoichiometry of 1 : 1.

The importance of donor influence on coordination mode is clearly demonstrated by the formation of the solvent-separated triple-ion [Mg(15-crown-5)(THF)$_2$][SMes*]$_2$ (Fig. 10),[42] isolated in quantitative yield when (Bu)$_2$Mg is reacted with two equivalents of the sterically demanding thiol HSMes* in the presence of crown-ether. In contrast, the monomeric distorted tetrahedral adduct Mg(SMes*)$_2$(Et$_2$O)$_2$ [25](Fig. 5) is formed if the reaction is carried out in diethylether and no crown-ether is present. [Mg(15-crown-5)(THF)$_2$SMes*]$_2$ [42] displays a seven-coordinate magnesium cation and two isolated thiolate anions. The magnesium and thiolate sulfur atom are separated by more than 6 Å.

Mg(SMes*)$_2$(OEt$_2$)$_2$ [25] displays a distorted tetrahedral geometry, with angles at magnesium ranging from 93.5(1)° to 140.4(1)°. The largest angle values are found between the two sterically demanding thiolato groups, the smallest between the two ether oxygen atoms. The closely related selenolate Mg(SeMes*)$_2$(THF)$_2$ [25] displays Mg–Se distances of

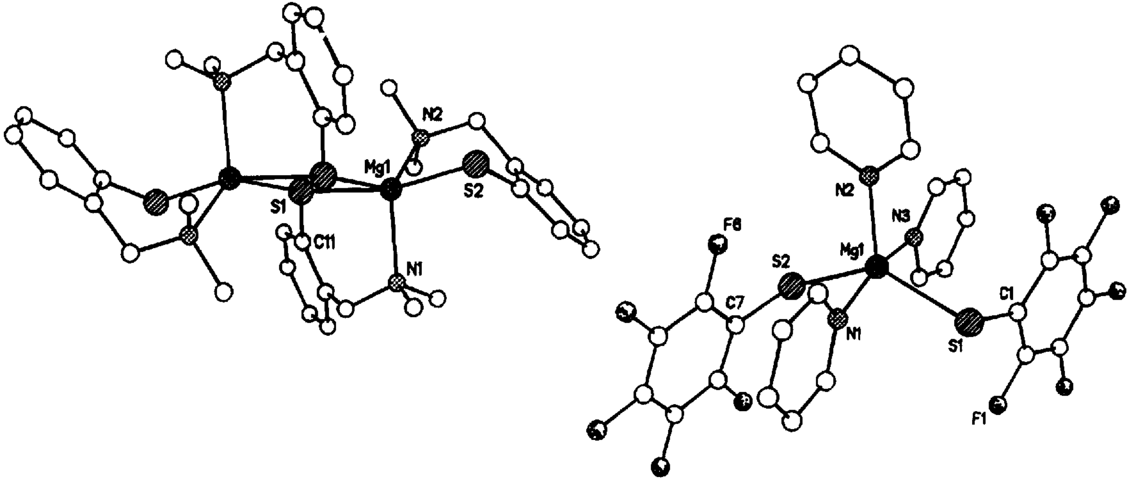

FIGURE 7 The crystal structures of $[Mg(SC_6H_4\text{-}2\text{-}CH_2NMe_2)_2]_2$ (Refs. 15 and 16) and $Mg(SC_6F_5)_2(py)_3$ (Ref. 42); hydrogen atoms have been omitted for clarity.

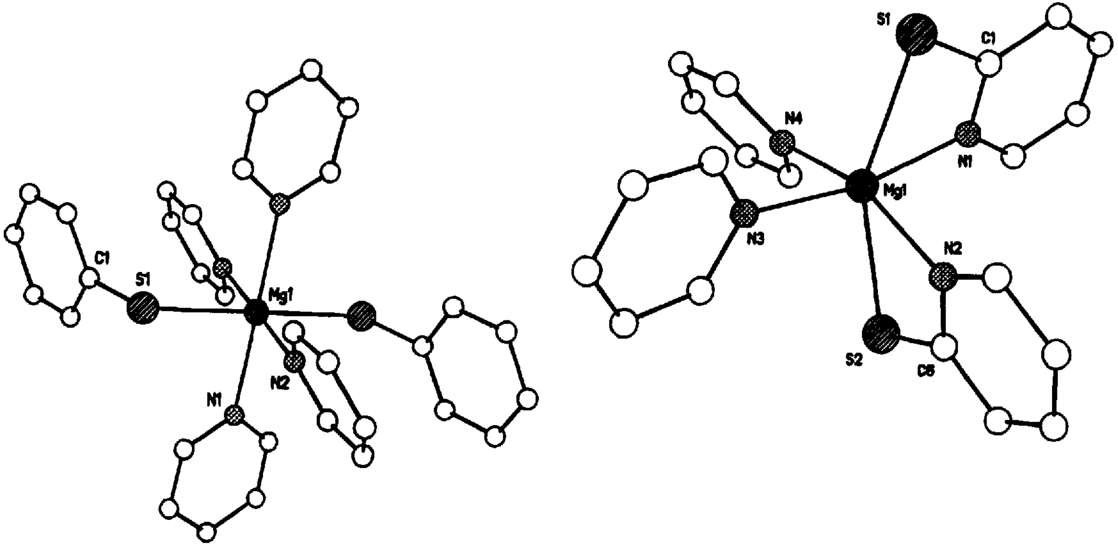

FIGURE 8 The crystal structures of $Mg(SPh)_2(py)_4$ (Ref. 42) and $Mg(S2\text{-}NC_5H_4)_2(py)_2$ (Ref. 42); hydrogen atoms have been omitted for clarity.

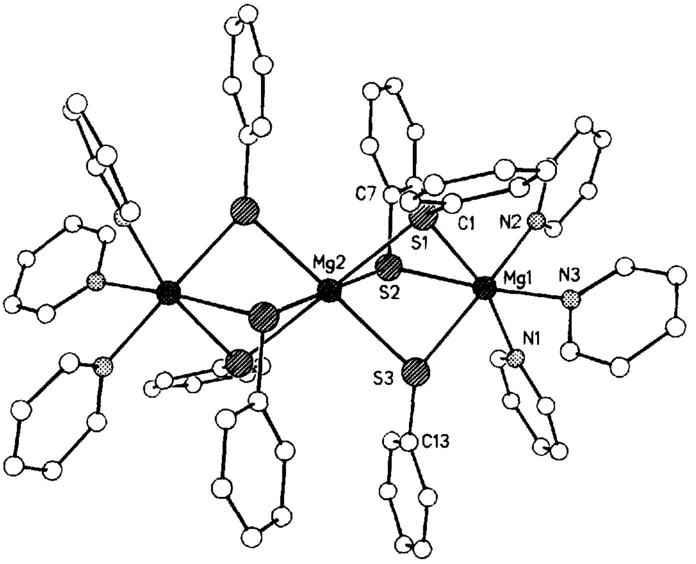

FIGURE 9 The crystal structure of the trimeric $[Mg_3(\eta^2SPh)_6(py)_6]$ (Ref. 42). Hydrogen atoms have been omitted for clarity.

2.526(3) and 2.539(3) Å, with angles at magnesium ranging between 97.4(2) Å and 122.1(1)°. Direct comparison of the solid state structures of $Mg(SMes^*)_2(Et_2O)_2$ and $Mg(SeMes^*)_2(THF)_2$ reveals similar structural features with different degrees of distortion from regular tetrahedral geometry, indicating the larger effective bulk of the thiolato versus the selenolato ligand. The reduced steric requirement of the selenolate ligand is due to the longer Mg–Se bond lengths (2.53(1) Å avg.) in comparison to the shorter Mg–S contacts (2.39(1) Å avg.).

A comparison of magnesium-sulfur contacts in the dimeric, three-coordinate $[Mg(STriph)_2]_2$ [25] (2.349(5) Å (terminal), 2.466(5) Å (bridging) with the hypothetical, monomeric, two-coordinate $Mg(SH)_2$ (2.324 Å) [55] reveals slightly longer bond lengths for the three coordinate compound. The increase of bond lengths with increasing coordination number is also observed for higher coordinate species, such as the four coordi-nate etherate $Mg(SMes^*)_2(OEt_2)_2$ (2.39(1) Å avg.). The experimentally determined Mg–S distances agree well with the sum of radii for four coordinate Mg^{2+} and S^{2-} (2.41 Å).[58] The four-coordinate magnesiate [lutidine $H]_2$ $[Mg(SC_6F_5)_4]$[42] exhibits average Mg–S distances of about

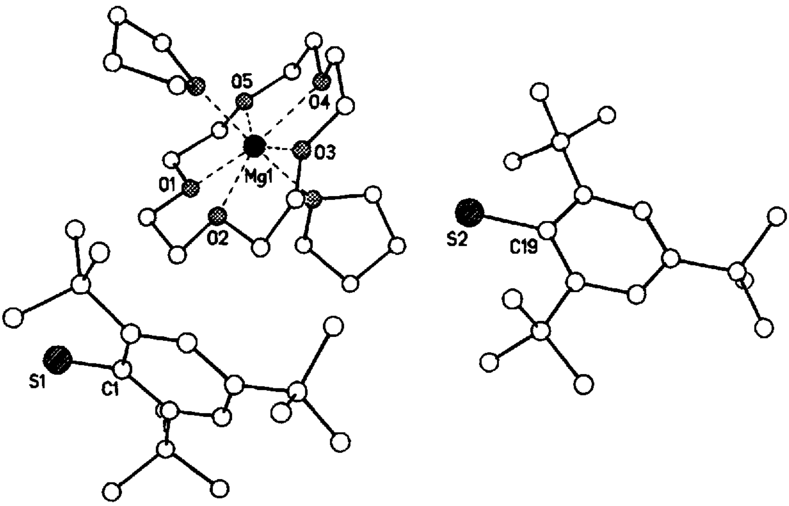

FIGURE 10 The crystal structure of the solvent-separated triple-ion [Mg(15-crown-5)$(THF)_2$][SMes*$]_2$ (Ref. 42). Hydrogen atoms have been omitted for clarity.

2.45(1) Å, which are slightly longer than in the neutral species, probably the result of increased repulsion due to two negative charges in the system. The magnesium selenium distances in Mg(SeMes*$)_2$ $(THF)_2$[25] (2.537(6) Å (avg.)) and Mg{SeSi$(SiMe_3)_3$$\}_2$TRMPSI[29] (2.49 (2) Å (avg.)) are very comparable; the slight differences can be rationalized by considering different steric requirements of the Si$(SiMe)_3$ versus the Mes* ligand. The relative increase in magnesium-sulfur to magnesium-selenium bond distances follows almost exactly the radius increase from sulfur to selenium.

Magnesium chalcogenolates with coordination numbers higher than four are obtained if the steric requirement of the ligand is reduced, as demonstrated with the intramolecularly stabilized five-coordinate dimer $[Mg(SC_6H_4\text{-}2\text{-}CH_2NMe_2)_2]_2$ [26] and the monomeric $Mg(SC_6F_5)_2(py)_3$ [42] (Fig. 7). In $[Mg(SC_6H_4\text{-}2\text{-}CH_2NMe_2)_2]_2$ each magnesium atom is ligated by three sulfur atoms, two bridging (2.548(2) Å avg.) and one terminal (2.446(2) Å). Additionally, each magnesium is coordinated to two nitrogen donors, resulting in a distorted pyramidal environment at magnesium. A similar coordination environment is observed for the monomeric $Mg(SC_6F_5)_2(py)_3$ with Mg–S distances of 2.476 and 2.505 Å. The distorted geometry of the monomeric species can be rationalized by invoking

VSEPR rules, assuming a distortion from trigonal bipyramidal geometry with the bulkier SC_6F_5 ligands in the equatorial plane, and the smaller pyridine donors in one equatorial and the two axial positions. The two neighboring fluorinated thiolate ligands repel each other, resulting in a widening of the S–Mg–S angle to 136.4(1)°. Simultaneously, the pyridine groups will distort from the axial positions towards the equatorial plane, resulting in a N(1)–Mg–N(3) angle of 168.6(1)°. The comparison of magnesium-sulfur bond length in the five-coordinate complexes with the sum of ionic radii for five-coordinate Mg^{2+} and S^{2-} (2.50 Å)[58] shows very similar values.

Magnesium thiolates exhibiting six coordinate metal centers become available if the ligand size is reduced further, as shown with the replacement of the pentafluorophenyl thiolate ligand by the slightly smaller phenylthiolate. Examples are the monomeric $Mg(SPh)_2(py)_4$,[42] the trimeric $[Mg_3(\eta^2SPh)_6(py)_6]$, or the pyridinethiolate species $Mg(S2\text{-}NC_5H_4)_2(py)_2$. The intramolecularly stabilizing pyridine thiolate ligand introduces a fair amount of steric strain into the system, whereas in $Mg(SPh)_2(py)_4$ or $[Mg_3(\eta^2SPh)_6(py)_6]$ an almost undistorted octahedral geometry at magnesium is observed. The magnesium-sulfur distances in the six-coordinate species are very similar with 2.635(1) Å for $Mg(SPh)_2(py)_4$, an average of 2.612 Å for the trimer and 2.612(1) Å (avg.) for $Mg(S2\text{-}NC_5H_4)_2(py)_2$. Surprisingly, the bridging nature of the thiolato groups in the trimer does not lead to an increase in Mg–S bond length, whereas slightly longer Mg–S distances are observed in the intramolecularly stabilized $Mg(S2\text{-}NC_5H_4)_2(py)_2$. The unusually short Mg–S distances in the trimer might be explained on the basis of the triply bridging of the nature of the thiolate groups, resulting in a shortening of magnesium-sulfur bond length.

The overall comparison of magnesium-sulfur bond lengths in the three-, four-, five-, and six-, coordinate magnesium thiolates follows the fairly straightforward trend: bond length increase with increasing coordination number. The good agreement between experimental Mg–S bond distances and the sum of ionic radii implies a substantial ionic character for the magnesium-sulfur bond, a view further supported by the facile formation of solvent-separated triple-ions.

The solvent-separated triple-ion $[Mg(15\text{-crown-}5)(THF)_2][SMes^*]_2$[42] is isolated in quantitative yield if crown-ether is present in the reaction mixture. Apparently, the strong magnesium-oxygen donor interactions are favored over the weaker-metal ligand contacts. The surprisingly stable compound displays a seven-coordinate magnesium cation and two isolated thiolate anions. A comparison of sulfur-carbon distances in $Mg(SMes^{*})_2(Et_2O)_2$[25] and $[Mg(15\text{-crown-}5)(THF)_2][SMes^{*}]_2$[43] shows slightly shorter contacts (1.772(2) Å avg.) for the solvent-separated triple-ion than in the contact molecule (1.803 (2) Å avg.). The shorter bonds can be explained by the reduced coordination number at sulfur.

3.3. Calcium Thiolates, Selenolates and Tellurolates

Published structural data of calcium chalcogenolates are limited to the tellurolate $Ca(TeSi(SiMe_3)_3)_2(THF)_4$ (Fig. 11a) published in 1992.[14,27,29] Recent work in our laboratory focusing on the development of facile, reliable synthetic routes to allow for the high yield preparation of calcium chalcogenolates resulted in the preparation and structural characterization of a small selection of calcium thiolates.[43] Table IV summarizes selected structural parameters of the calcium target molecules.

The commonly observed coordination geometry in calcium chalcogenolates seems to contain six or more ligands as observed in the monomeric octahedral pyridine adduct $Ca(SC_6F_5)_2(py)_4$[43] (Fig. 11b), the unusual six-coordinate mixed thiolate hydroxide dimer [Ca(SMes*

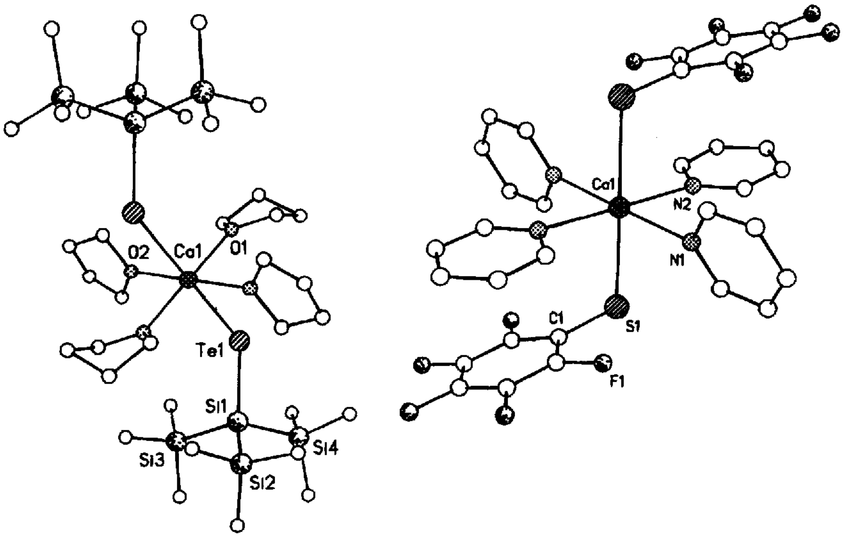

FIGURE 11 The crystal structures of $Ca(TeSi(SiMe_3)_3)_2(THF)_4$ (Refs. 14 and 27) and $Ca(SC_6F_5)_2(py)_4$ (Ref. 43); hydrogen atoms have been omitted for clarity.

TABLE IV

Selected structural parameters for calcium chalcogenolates.

Compound	Ae-E (Å)	Ae-Donor (Å)	S-C_{ipso} (Å)	C. N. (metal)	Ref.
$Ca(SC_6F_5)_2(py)_4$	2.8493(4)	2.502(2), 2.534(2)	1.752(2)	6	43
[CaSMes*(η^2-OH) PMDTA]$_2$	2.836(1)	2.598(3), 2.644(3) 2.692(3)	1.782(3)	6	43
[Ca(SMes*)$_2$ (18-crown-6)]	2.785(2), 2.859(2)	2.527(5), 2.545(5) 2.587(5), 2.622(5) 2.625(5), 2.632(5)	1.768(7), 1.796(7)	8	43
[Ca(18-crown-6) $(NH_3)_3$][SMes*]$_2$	–	2.469(3)–2.541(2)^a 2.461(3)–2.781(3)^b	1.761(4), 1.775(4)	9	43
$Ca(TeSi(SiMe_3)_3)_2$ $(THF)_4$	3.197(1)	2.363(2), 2.401(2)	2.483(1)	6	14, 27, 29

Abbreviations: Mes* = 2,4,6-$tBu_3C_6H_2$, py = pyridine, PMDTA = N, N, N′, N′, N″, N″ pentamethyldiethylenetriamine.

[a] $Ca–NH_3$ contacts.

[b] Ca–crown-ether contacts.

(μ-^{2}OH)PMDTA]$_2$[43] (PMDTA = N, N, N′, N′, N″, N″ pentamethyldiethylenetriamine), the eight-coordinate crown-ether derivative Ca(18-crown-6)(SMes*)$_2$[43] (Fig. 12) or the solvent-separated triple-ion [Ca(18-crown-6)$(NH_3)_3$] [SMes*]$_2$ [43] (Fig. 13) displaying a coordination number of nine at calcium. Since only a few calcium thiolates and tellurolates have been structurally examined, a general understanding of ligand and donor influence on structural chemistry is difficult to obtain. However, a comparison between structurally related magnesium and strontium analogues sheds some light on the coordination chemistry of the target molecules.

Calcium thiolates are mainly prepared by two synthetic routes, transamination and metallation (see Table I). The unusual mixed thiolate hydroxide, [Ca(SMes*)(μ-^{2}OH)PMDTA]$_2$[42] was synthesized employing transamination procedures; the hydroxide group was introduced by partial hydrolysis of the bisthiolate. The crown-ether derivatives, Ca(18-crown-6)(SMes*)$_2$ [Ca(18-crown-6)$(NH_3)_3$][SMes*]$_2$, were synthesized employing metallation procedures. The contact pair Ca(18-crown-6)(SMes*)$_2$ is available

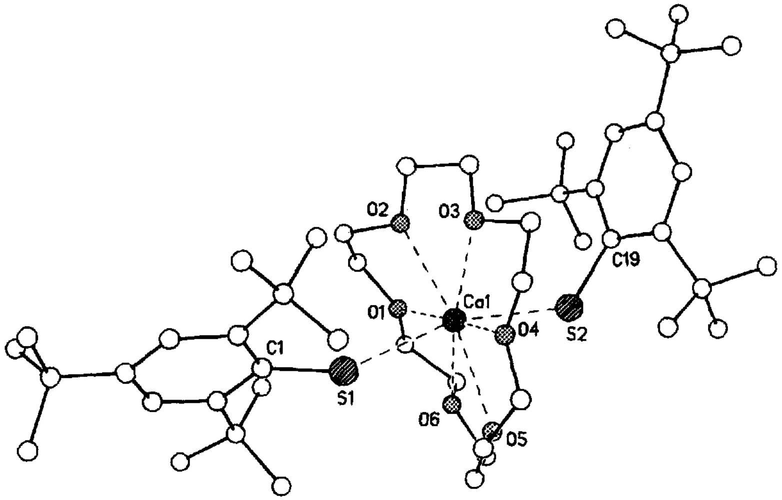

FIGURE 12 The crystal structure of Ca(SMes*)$_2$(18-crown-6) (Ref. 43); hydrogen atoms have been omitted for clarity.

from the solvent-separated derivative by brief refluxing in vacuum, resulting in the removal of the NH_3 donors and formation of the calcium-sulfur bonds. The tellurolate Ca(TeSi(SiMe$_3$)$_3$)$_2$(THF)$_4$ was synthesized using transamination procedures.[14,17]

Ca(SC$_6$F$_5$)$_2$(py)$_4$, shown in Fig. 11b, displays a perfectly octahedral coordination sphere, with a center of symmetry located at the metal center. The calcium-sulfur distances are 2.8494 Å, and the calcium nitrogen contacts are almost identical with 2.502 and 2.534 Å. The overall structural features are very similar to those of Mg(SPh)$_2$(py)$_4$; however, employment of the sterically more encumbered pentafluorophenylthiolate ligand results in the formation of the five coordinate Mg(SC$_6$F$_5$)$_2$(py)$_3$.[42] Apparently, the larger size of calcium allows the accommodation of two pentafluorothiolate ligands in addition to four pyridine donors. The octahedral species Ca(SC$_6$F$_5$)$_2$(py)$_4$ and [Ca(SMes*)η-^{2}OH)PMDTA]$_2$ display fairly similar calcium-sulfur distances of 2.849(1) and 2.836 (1) Å. These values fit closely with the calculated calcium-sulfur distances obtained by addition of the ionic radii of Ca^{2+} and S^{2-}, [58] but are significantly longer than the calcium-sulfur distance calculated by Pappas for the hypothetical, monomeric, two coordinate Ca(SH)$_2$ (2.650 Å).[55] This discrepancy can be explained on the basis of increased coordination

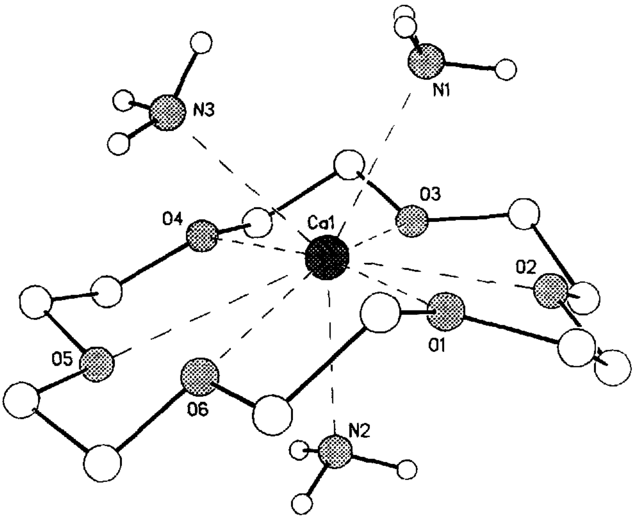

FIGURE 13 The crystal structure of the solvent-separated triple-ion [Ca(18-crown-6)(NH$_3$)$_3$][SMes*]$_2$ (Ref. 43). Only the cation is shown; hydrogen atoms, except those on ammonia, have been omitted for clarity.

numbers in the target molecules. Ca(18-crown-6)(SMes*)$_2$ displays an eight-coordinate calcium center with six calcium-oxygen and two calcium-sulfur contacts; interestingly, shorter calcium-sulfur bond lengths are observed for the eight-coordinate crown-ether derivative as compared to the six-coordinate pyridine adduct Ca(SC$_6$F$_5$)$_2$(py)$_4$.[43] This surprising result may be explained on the basis of weak, long Ca–O crown-ether distances (2.59 Å avg.) reducing the coordinative saturation effect of the crown-ether donor. Shorter, stronger Ca–O distances are observed in Ca(TeSi(SiMe$_3$)$_3$)$_2$(THF)$_4$ (2.363 and 2.410 Å).[14,29]

The solvent-separated triple-ion [Ca(18-crown-6)(NH$_3$)$_3$][SMes*]$_2$ [43] exhibits a nine-coordinate calcium center, with two NH$_3$ molecules on one face of the crown-ether and one NH$_3$ on the other; the crown-ether is bent towards the face which accommodates only one NH$_3$ donor (Fig. 3). This distortion is in accord with slight differences in calcium-nitrogen distances; the shortest contact is observed at the face with binds only one NH$_3$. The calcium nitrogen distances (2.469, 2.525 and 2.541 Å) are in the same range as those observed for Ca(SC$_6$F$_5$)$_2$(py)$_4$ and [Ca(SMes*)(μ-^{2}OH)PMDTA]$_2$. The calcium-oxygen crown-ether distances vary significantly from 2.421 up to 2.781 Å, indicating that calcium is not located symmetrically in the crown-ether donor. This is not a surprising result considering the high coordination number at calcium. The comparison of carbon-sulfur bond length in the solvent-separated triple-ion [Ca(18-crown-6)$(NH_3)_3$][SMes*]$_2$ and Ca(18-crown-6)(SMes*)$_2$ shows no significant deviations, which would indicate an increased bond order between carbon and sulfur in the solvent-separated species. Additionally, the anion shows no indication of delocalization of electron density into the phenyl ring. The slightly shorter C–S distance in the solvent-separated molecule is solely due to the smaller coordination number at sulfur.

3.4. Strontium Thiolates and Selenolates

Only a small collection of well-characterized strontium chalcogenolate derivatives has been reported.[28,29] Recent work in our laboratory added to this collection the solvent-separated strontium thiolate [Sr(18-crown-6)(HMPA)]$_2$[SMes*]$_2$,[44] shown in Fig. 14. Table V summarizes selected structural parameters.

Strontium chalcogenolates have been synthesized using a variety of synthetic routes, namely salt elimination reactions for the Sr(EMes*)$_2$(THF)$_4$ (E = S, Se),[28] transamination for Sr(SeSi(SiMe$_3$)$_3$)$_2$ (TMEDA)$_2$[29] and metallion for [Sr(18-crown-6)(HMPA)]$_2$[SMes*]$_2$.[44]

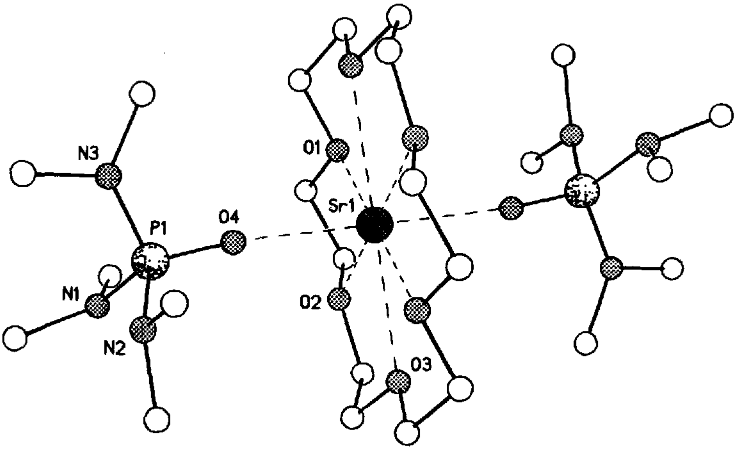

FIGURE 14 The crystal structure of the solvent-separated triple-ion [Sr(18-crown-6)(HMPA)$_2$][SMes*]$_2$ (Ref. 44). Only the cation is shown; hydrogen atoms have been ommitted for clarity.

TABLE V

Selected structural parameters for strontium chalcogenolates.

Compound	Ae-E (Å)	Ae-Donor (Å)	S-C$_{ipso}$ (Å)	C. N. (metal)	Ref.
Sr(SMes*)$_2$(THF)$_4$	2.951(2)	2.574(7), 2.565(7)	1.794(9)	6	28
[Sr(18-crown-6)(HMPA)$_2$][SMes*]$_2$		2.420(2)[a] 2.712(1), 2.718(1) 2.736(1)[b]	1.771(2)	8	44
Sr(SeMes*)$_2$(THF)$_4$	3.066(1)	2.590(7), 2.536(7)	1.946(8)	6	28
Sr(SeSi(SiMe$_3$)$_3$)$_2$ (TMEDA)$_2$	2.946(1)	2.69(1), 2.69(1)	2.235(3)	6	29

Abbreviations: TMEDA = N,N,N′,N′-tetramethylethylenediamine, HMPA = Hexamethylphosphoramide, py = pyridine, Mes* = 2,4,6-tBu$_3$C$_6$H$_2$.

[a] Sr–HMPA contacts.

[b] Sr–crown-ether contacts.

The octahedrally coordinate strontium derivatives Sr(SMes*)$_2$THF$_4$,[28] Sr(SMes*)$_2$THF$_4$[28] (Fig. 15) and Sr(SeSi(SiMe$_3$)$_3$)$_2$ (TMEDA)$_2$[29] display very similar structural motifs. The central Sr atom is surrounded in an octahedral fashion by two sterically encumbered chalcogenolate ligands, located *trans* to each other, in addition to four THF oxygen atoms or four TMEDA nitrogen donors, respectively. The strontium-sulfur distance of 2.951(1) Å in Sr(SMes*)$_2$THF$_4$ agrees well with the Sr–S bond distance observed in SrS$_2$C$_4$N$_2$·5 H$_2$O.[59] The slight differences (2.951(2) vs. 2974(4) Å) can be explained by the larger coordination number in SrS$_2$C$_4$N$_2$·5 H$_2$O[59](7 + 2 vs. 6). These strontium-sulfur distances are also fairly close to the sum of ionic radii of Sr^{2+} and S^{2-} (3.02 Å).[58] The strontium-selenium distances in Sr(SeSi(SiMe$_3$)$_3$)$_2$ (TMEDA)$_2$ and Sr(SeMes*)$_2$(THF)$_4$ differ only slightly (2.946 Å vs. 3.066 Å), explainable on the basis of reduced steric bulk of the -SeSi(SiMe$_3$)$_3$)$_2$ ligand as compared to -SeMes*. The novel solvent-separated [Sr(18-crown-6) (HMPA)$_2$][SMes*]$_2$ displays an eight-coordinate strontium cation, ligated by six crown-ether oxygen atoms and two HMPA oxygen donors. The cations and anions are separated by more than 6 Å. Apparently, the interaction of the strontium dication with crown-ether and the strong donor HMPA donor is sufficient to stabilize the large cationic metal center. The strontium-oxygen HMPA distances are 2.420(1) Å, in contrast, the strontium-oxygen crown-ether distances are much longer (2.722 Å avg.). Interestingly, the strong donor HMPA is needed to allow

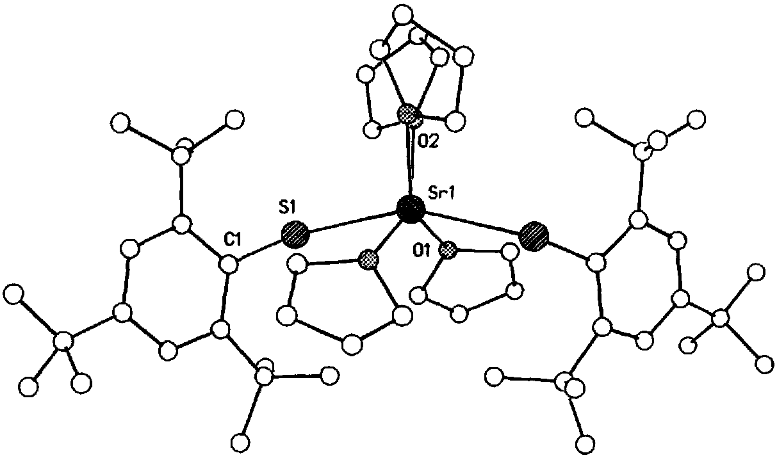

FIGURE 15 The crystal structure of $Sr(SMes^*)_2(THF)_4$ (Ref. 28); hydrogen atoms have been omitted for clarity.

for the isolation of this solvent-separated triple-ion; if reaction conditions are chosen similar to those employed for $[Ca(18\text{-crown-}16)(NH_3)_3][SMes^*]_2$,[42] an insoluble product is formed. Apparently, the strong donor characteristics and substantial partial negative charge on the oxygen of HMPA[54] is needed to stabilize the large, strontium center.

3.5. Barium Thiolates, Selenolates and Tellurolates

The number of well-characterized barium chalcogenolates is very small; to date the structural characterization of a single compound, $Ba(TeSi(SiMe_3)_3)_2(py)_5$[29] has appeared in the literature. Recent work in our laboratory, concerned with the development of a facile access route to alkaline-earth chalcogenolates, enabled the synthesis and structural characterization of a small number of barium thiolates and selenolates. Table VI summarizes selected structural data.

Examples of structurally characterized barium chalcogenolates are limited to one thiolate species, which became available employing metallation procedures. [Ba(SMes*)(18-crown-6)(HMPA)][SMes*] (Fig. 16) exhibits a monocationic barium center, ligated to only one (SMes*) ligand in addition to the donors 18-crown-6 and HMPA. Charge neutrality is maintained by one free thiolate anion $[SMes^*]^-$ (Fig. 16). The barium center and sulfur atom from the free thiolate ligand are separated by more

TABLE VI

Selected structural parameters for barium chalcogenolates.

Compound	Ae-E (Å)	Ae-Donor (Å)	S-C_{ipso} (Å)	C. N. (metal)	Ref.
[Ba(SMes*)(HMPA)] [SMes*]	3.012(1)	2.773(1)– 2.808(1)	1.803(1), 1.781(1) 1.754(1), 1.776(1)	8	45
Ba(SeMes*)$_2$(THF)$_4$	3.288(1)	2.744(3), 2.745(3)	1.933(3)	6	45
[Ba(SeTrip)$_2$(py)$_3$ (THF)]$_2$	3.297(1), 3.277(1) 2.419(1)	2.874(1), 2.906(1) 2.8234(1), 2.823(1) (O)	1.943(1), 1.935(1)	7	45
Ba(SeTrip)$_2$ (18-crown-6)	3.229(1), 3.230(1)	2.773(4)– 2.792(4)	1.936(6), 1.926(6)	8	45
Ba(TeSi(SiMe$_3$)$_3$)$_2$ (py)$_5$	3.382(1)	2.934(5), 2.856(4) 2.874(3)	2.467(1)	7	29

Abbreviations: HMPA = Hexamethylphosphoramide, py = pyridine, Mes* = 2,4,6-tBu$_3$C$_6$H$_2$, Trip = 2,4,6iPr$_3$C$_6$H$_2$.

than 6 Å. The thiolate derivative displays an interesting structural motif: an intermediate structure between contact and solvent-separated ion. Interestingly, the molecule was synthesized and crystallized utilizing excess HMPA, expecting the formation of a solvent-separated species analogous to the strontium derivatives. Instead, the monocationic species was observed. Attempts to synthesize the contact pair, displaying two barium-sulfur bonds analogous to the calcium derivative Ca(SMes*)$_2$(18-crown-6), were not successful; apparently, the tight crown-ether coordination at barium induces a significant steric shield, making it impossible to accommodate two large thiolate ligands at barium. It is believed that the barium-sulfur bond strength seems to slightly exceed the barium-oxygen HMPA donor interaction; the formation of the intermediate seems to be a compromise between steric and bond strength effects. The Ba–S bond length of 3.012(1) Å is slightly shorter thatn the sum of ionic radii.[58] Apparently, the cationic nature of the compound causes the shortening of the barium-sulfur bond. However, the experimental barium-sulfur bond length agrees well with the barium-sulfur distances observed in the tetrasulfide derivative BaS$_4$(18-crown-6)DMF.[45]

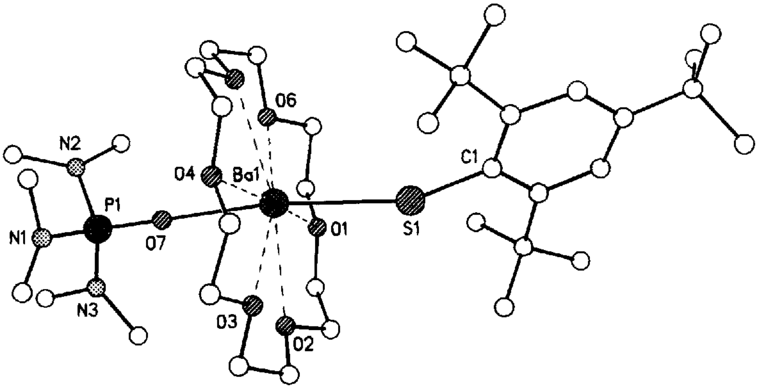

FIGURE 16 The crystal structure of [Ba(SMes*)(18-crown-6)(HMPA)][SMes*] (Ref. 45). Only the cation is shown; hydrogen atoms have been removed for clarity.

A small group of barium selenolates, the seven coordinate [Ba{η^1 SeTrip}{η^2SeTrip}(py)$_3$(THF)]$_2$ (Fig. 17), the eight coordinate crown-ether derivative Ba(SeTrip)$_2$(18-crown-6), and the distorted octahedrally coordinate Ba(SeMes*)^2(THF)$_4$, which is isostructural with the corresponding strontium derivative,[28] became available by reacting the corresponding diselenides with barium metal in liquid, dry ammonia. With the synthesis of these compounds it was shown for the first time that alkaline-earth insertion into the Se–Se bond results in the clean formation of the target molecules (see Table I). A comparison of coordination geometries of the barium target molecules with the lighter alkaline-earth congeners indicates the pronounced tendency for the formation of higher coordination numbers, an expected trend, considering the significant increase in ionic radius. The isolation of the six coordinate Ba(SEMe*)$_2$ (THF)$_4$, E = S, Se isostructural to Sr(SEMes*)$_2$(THF)$_4$ [28] was possible by employment of the sterically demanding SEMes* ligand. Reduction of the ligand size and employment of the smaller SeTrip ligand led to the isolation of the seven coordinate dimer [Ba{η^1SeTrip}{η^2SeTrip} (py)$_3$(THF)]$_2$ (Fig. 17), and the eight coordinate crown-ether derivative [Ba(SeTrip)$_2$ (18-crown-6). A comparison of Ba–Se distances for all three compounds reveals very similar values; except for one bridging contact in the dimer, distances of 3.288(1) Å for the six coordinate Ba(SeMes*) (THF)$_4$ 3.297(1) and 3.277(1) Å for the dimer and 3.229(1) and 3.230(1) Å for Ba(SeTrip)$_2$ (18-crown-6) are observed. Interestingly, the shortest contacts are displayed for the eight coordinate crown-ether derivative, a trend previously

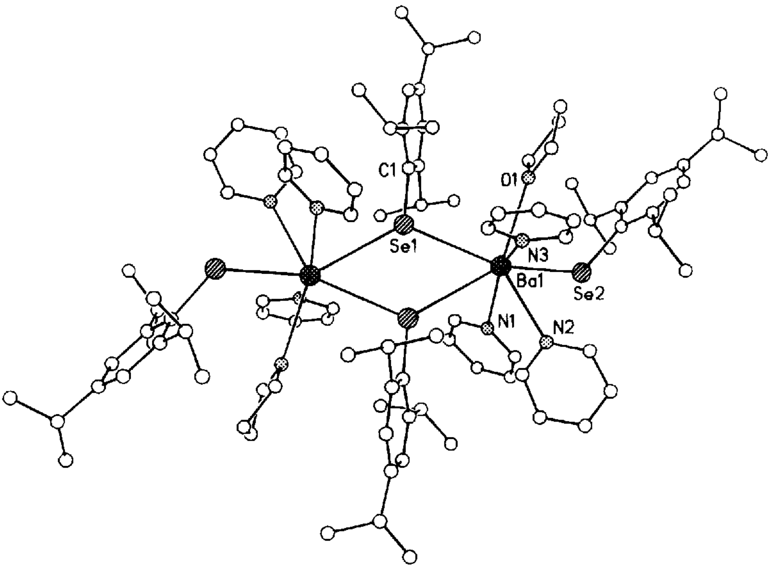

FIGURE 17 The crystal structure of Ba $\{\eta^1\text{SeTrip}\}\{\eta\ ^2\text{SeTrip}\}(\text{py})_3(\text{THF})]^2$ (Ref. 45). Hydrogen atoms have been omitted for clarity.

seen in the related calcium species.[43] This result might be explained by the reduced size of the selenolate ligand. The barium-selenium bond length is in good accord with the sum of ionic radii for Ba^{2+} and Se^{2-}.[58]

SUMMARY

During the last few years, progress in alkaline-earth chalcogenolate chemistry has been significant. Numerous synthetic routes have been explored, allowing for the synthesis of a variety of target molecules. This work included the investigation of ligand and donor influence on structural features, and is currently concerned with the correlation of structural aspects with important properties such as solubility, volatility and reactivity.

In the past, progress in alkaline-earth chemistry has been hampered by the lack of suitable synthetic procedures and the formation of polymeric, intractable materials. The use of sterically demanding ligands, often in combination with donors, allowed the synthesis of non-polymeric, soluble species, which were subjected to a variety of analytical methods, resulting in an improved understanding of metal-chalcogen bond characteristics. It has been shown that the coordination number displayed by the complexes can clearly be influenced by ligand and donor choice. Apparently, the ligand has the larger influence in determining the overall structural features of the complexes, as shown with the five-coordinate $Mg(SC_6F_5)_2(py)_3$ and the six-coordinate $Mg(SPh)_2(py)_4$; here the smaller size of the thiolato ligands is responsible for the formation of the octahedral species. However, it has been shown that donor influence is critical as well, especially if multidentate donors such as crown-ether are employed. The easy formation of solvent-separated triple-ions in the presence of crown-ethers and/or very strong donors as observed for all alkaline-earth elements indicates the high ionic bond character in alkaline-earth chalcogenolates.

Our improved knowledge of synthetic strategies and structure-determining factors has paved the way for the use of the target molecules as reagents and precursors for technically important materials. With a variety of synthetic methodologies in hand, we will continue our work with the exploration of decomposition mechanism and the production of mixed group II–VI semiconductor materials. The usefulness of magnesium chalcogenolates in synthetic applications will also be further investigated.

Acknowledgments

I would like to thank my co-workers Ulrich Englich, Scott Chadwick, David Green and Sona Dalal for their enthusiasm and hard work over the last three years, which made this article possible! I would also like to thank Dr. Mathias O. Senge (Freie Universität Berlin) and Dr. Bruce Noll (University of Colorado at Boulder) for the collection of selected crystallographic data and Professor Anthony L. Spek (Utrecht University) for the structural data of $[Mg(SC_6H_4\text{-}2\text{-}CH_2NMe_2)_2]_2$.

Acknowledgment for financial support of this research is made to the National Science Foundation, the donors of the Petroleum Research Fund, administered by the American Chemical Society, the Deutsche Forschungsgemeinschaft for a postdoctoral stipend to U.E., the W. M. Keck Foundation, and Syracuse University.

References

1. *Physics and Material Science of High Temperature Superconductors*, R. Kossowski, S. Methfessel, D. Wohlleben, Eds., NATO ASI Series E, Vol. 181, Kluwer Academic Publishers.
2. J. G. Bednorz, K. A. Muller, M. Takashige, *Science*, **236**, 73 (1987).

3. R. J. Cova, B. Batlogg, R. B. Van Dover, P. W. Murphy, S. Sunshine, T. Siegrist, J. P. Remeika, E. A. Reitman, S. Zahvrak, G. P., Espinosa, *Phys. Rev. Lett.* **58**, 1676 (1987).
4. L. G. Hubert-Pfalzgraf, *New Journal of Chemistry*, **11**, 663 (1987).
5. D. C. Bradley, *Chem. Rev.* **89**, 1317 (1989).
6. K. G. Caulton, L. G. Hubert Pfalzgraf, *Chem. Rev.* **90**, 969 (1990).
7. See for example: (a) P. J. Hamson, T. J. Leedham, *Chemtronics*, **5**, 115 (1991); (b) K. G. Caulton, M. H. Chisholm, S. R. Drake, K. Folting, J. C. Huffman, W. S. Streib, *Inorg. Chem.* **32**, 1970 (1993); (c) S. R. Drake, W. S. Streib, M. H. Chisholm, K. G. Caulton, *Inorg. Chem.* **29**, 2708 (1990); (d) K. G. Caulton, M. H. Chisholm, S. R. Drake, K. Folting, *J. Chem. Soc. Chem. Commun.* 13349, (1990); (e) K. G. Caulton, M. H. Chisholm, S. R. Drake, W. S. Streib, *Angew. Chem. Int. Ed. Engl.* **29**, 1483 (1990); (f) W. Bidell, H. W. Bosch, D. Veghini, H. U. Hund, J. Döring, H. Berke, *Helv. Chim. Acta*, **76**, 596 (1993); (g) S. R. Drake, S. A. S. Miller, D. J. Williams, *Inorg. Chem.* **32**, 3227 (1993); (h) S. R. Drake, M. B. Hursthouse, K. M. A. Malik, S. A. S. Miller, D. J. Otway, *Inorg. Chem.* **32**, 4464 (1993); (i) W. S. Rees Jr., W. W. Carris, W. Hesse, *Inorg. Chem.* **30**, 4481 (1991); (j) J. A. Darr, S. R. Drake, D. J. Williams, A. M. Z. Slawin, *J. Chem. Soc. Chem. Commun*, 866, (1993); (k) S. R. Drake, M. B. Hursthouse, K. M. A. Malik, S. A. S. Miller, *J. Chem. Soc. Chem. Commun*, 478, (1993); (l) S. R. Drake, M. B. Hursthouse, K. M. A. Malik, D. J. Otway, *J. Chem. Soc., Dalton Trans.* 2882 (1993); (m) A. P. Purdy, A. D. Berry, R. T. Holm, M. Fatemi, D. K. Gaskill, *Inorg. Chem.* **28**, 2799 (1989); (n) S. K. Pandey, A. Steiner, H. W. Poesky, D. Stalke, *Angew. Chem.* **105**, 625 (1993); (o) S. R. Drake, M. B. Hursthouse, K. M. A. Malik, S. A. S. Miller, *Inorg. Chem.* **32**, 4652 (1993); (p) W. S. Rees. Jr., C. R. Caballero, W. Hesse, *Angew. Chem. Int. Ed. Engl.* **31**, 735 (1992).
8. H. Okuyama, K. Nakano, T. Miyajima, K. Akimoto, *Jpn. J. Appl. Phys.* **30**, L1620 (1991).
9. K. Kondo, H. Okuyama, A. Ishibashi, *Appl. Phys. Lett.* **64**, 3434 (1994).
10. J. Suda, Y. Kawakami, S. Fujita, *Jpn. J. Appl. Phys.* **33**, L290 (1994).
11. K. Kondo, M. Ukita, H. Yshida, Y. Kishita, H. Okuyama, S. Ito, T. Ohata, K. Nakano, *J. Appl. Phys.* **76**, 2621 (1994).
12. (a) C. K. Lowe-Ma, T. A. Vanderah, T. E. Smith, *J. Solid State Chem.* **117**, 363 (1995); (b) P. N. Kumta, S. H. Risbid, *J. Mater. Sci.* **29**, 1135 (1994).
13. M. M. Yuta, W. B. White, *J. Electrochem. Soc.* **139**, 2347 (1992) .
14. D. E. Gindelberger, J. Arnold, *J. Am. Chem. Soc.* **114**, 6242 (1992).
15. D. M. Knotter, W. J. J. Smeets, A. L. Spek, G. van Koten, *J. Am. Chem. Soc.* , **112**, 5895 (1990).
16. This review article summarizes the small selection of published magnesium thiolates and discusses their use in synthetic applications. M. D. Janssen, D. M. Grove, G. van Koten, *Progress in Inorganic Chemistry*, K. Karlin, Editor, in press.
17. P. J. Wright, B. Cockayne, *Chemtronics*, 49, (1987).
18. J. O. Williams, *Chemtronics*, 43, (1987).
19. P. O'Brien, *Chemtronics*, 62, (1991).
20. *Semiconductor Materials*, L. I. Berger, Ed., CRC Press, Boca Raton, (1996).
21. A. F. Wells, *Structural Inorganic Chemistry*, Oxford Science Publications, Fifth Edn. (1984).
22. F. M. McDonnell, K. Ruhlandt-Senge, J. J. Ellison, R. H. Holm, P. P. Power, *Inorg. Chem.* **34**, 1815 (1995).
23. This recent review article summarizes progress in selenolate and tellurolate chemistry, mentioning published alkaline-earth selenolates and tellurolates. J. Arnold, *Progress in Inorganic Chemistry*, V 43, p. 353, K. Karlin, Editor, Wiley, (1995).
24. K. Ruhlandt-Senge, R. A. Bartlett, M. M. Olmstead, P. P. Power, *Inorg. Chem.* **32**, 1724 (1993).
25. K. Ruhlandt-Senge, *Inorg. Chem.* **34**, 3499 (1995).

26. M. D. Jannsen, R. van der Rist, A. L. Spek, D. M. Grove, G. van Koten, *Inorg. Chem.* **35**, 3436 (1996).
27. G. Becker, K. W. Klinkhammer, W. Schwarz, M. Westerhausen, T. Hildenbrand, *Z. Naturforsch*, **47B**, 1225 (1992).
28. K. Ruhlandt-Senge, K. Davis, S. Dalal, U. Englich, M. O. Senge, *Inorg. Chem.* **34**, 2587 (1995).
29. D. E. Gindelberger, J. Arnold, *Inorg. Chem.* **33**, 6293 (1994).
30. N. A. Bell, *Comprehensive Organometallic Chemistry*, G. Wilkinson, F. G. A. Stone and E. W. Abel, Editors, Pergamon Press, Oxford, (1982).
31. W. E. Lindsell, in *Comprehensive Organometallic Chemsitry*, G. Wilkinson, F. G. A. Stone and E. W. Abel, Editors, Pergamon Press, Oxford, (1982).
32. T. P. Hanusa, *Acc. Chem. Res.* **93**, 1023 (1993).
33. T. P. Hanusa, *Polyhedron* **9**, 1345 (1990).
34. J. Calabrese, M. A. Cushing, Jr., D. Ittel, *Inorg. Chem.* **27**, 867 (1988).
35. P. B. Hitchcock, M. F. Lappert, G. F. A. Lawless, B. Royo, *J. Chem. Soc., Chem. Commun.* 1141, (1990).
36. J. A. Darr. S. R. Drake, M. B. Hursthouse, K. M. A. Malik, *Inorg. Chem.* **32**, 5704, (1993).
37. K. G. Caulton, M. H. Chisholm, S. R. Drake, K. Folting, *J. Chem. Soc., Chem. Commun.* 1349, (1990).
38. K. G. Caulton, M. H. Chisholm, S. R. Drake, W. E. Streib, *Angew. Chem. Int. Ed. Engl.* **29**, 1483 (1990).
39. S. R. Drake, W. E. Streib, K. Folting, K. J. Caulton, M. H. Chisholm, *Inorg. Chem* **31**, 3205, (1993).
40. *Gmelin Handbook of Chemistry*, Gmelin Verlag, Frankfurt.
41. S. Chadwick, U. Englich, K. Ruhlandt-Senge, in preparation.
42. S. Chadwick, U. Englich, K. Ruhlandt-Senge, in preparation.
43. S. Chadwick, U. Englich, K. Ruhlandt-Senge, in preparation.
44. U. Englich, S. Chadwick, K. Ruhlandt-Senge, in preparation.
45. S. Chadwick, U. Englich, K. Ruhlandt-Senge, in preparation.
46. (a) J. M. Boncella, C. J. Coston, J. K. Cammack, *Polyhedron*, **10**, 769 (1991); (b) B. A. Vaarstra, J. C. Huffman, W. E. Streib, K. G. Caulton, *Inorg. Chem.* **30**, 121 (1991); (c) M. Westernhausen, *Inorg. Chem.* **30**, 96 (1991).
47. U. Englich, K. Ruhlandt-Senge, in preparation.
48. M. Brewer, D. Khasnis, M. Bureta, M. Beraldini, T. J. Emge, J. G. Brennan, *Inorg. Chem.* **33**, 2743 (1994).
49. (a) M. L. Steigerwald, C. R. Sprinkle, *J. Am. Chem. Soc.* **109**, 7200 (1987); (b) J. Arnold, J. M. Walker, K. M. Yu, P. J. Bonasia, A. L., Seligson, E. D. Bourret, *J. Cryst. Growth* **124**, 647 (1992).
50. W. Rundel, *Chem. Ber.* **101**, 2956 (1968).
51. D. N. Skilleter, *Chem. Br.* **26**, 26 (1990).
52. F. H. Allen, J. E. Davies, J. J. Galloy, O. Johnson, O. Kennard, C. F. Macrae, E. M. Mitchell, G. F. Mitchell, J. M. Smith, D. G. Watson, "The Cambridge Structural Database," *J. Chem. Info. Sci.* **31**, 187 (1991).
53. H. Nöth, D. Schlosser, *Chem. Ber.* **121**, 1711, (1988).
54. D. R. Armstrong, S. Bennet, M. G. Davisson, R. Snaith, D. Stalke, D. S. Wright, *J. Chem. Soc. Chem. Commun.* 262, (1992).
55. J. A. Pappas, *J. Am. Chem. Soc.* **100**, 6023 (1978).
56. J. J. Ellison, P. P. Power, *Inorg. Chem.* **33**, 4321 (1994).
57. P. Ghosh, G. Parkin, *Chem. Commun.* 1239 (1996).
58. J. E. Huheey, E. A. Keiter, R. L. Keiter, *Inorganic Chemistry*, 4th Edn., Harper Collins, (1993).
59. H. U. Hummel, C. Wolf, *Z. Naturforsch.* **41b**, 1206 (1986).